

Measuring Quark-Gluon-Plasma Thermalization Time with Dileptons

Mauricio Martinez¹ and Michael Strickland²

¹*Helmholtz Research School*

Johann Wolfgang Goethe - Universität Frankfurt

Ruth-Moufang-Straße 1, D-60438 Frankfurt am Main, Germany

²*Institut für Theoretische Physik and Frankfurt Institute for Advanced Studies*

Johann Wolfgang Goethe - Universität Frankfurt

Max-von-Laue-Straße 1, D-60438 Frankfurt am Main, Germany

We calculate the medium dilepton yield from a quark-gluon plasma which has a time-dependent momentum-space anisotropy. A phenomenological model for the hard momentum scale, $p_{\text{hard}}(\tau)$, and plasma anisotropy parameter, $\xi(\tau)$, is constructed which interpolates between longitudinal free streaming at early times ($\tau \ll \tau_{\text{iso}}$) and ideal hydrodynamic at late times ($\tau \gg \tau_{\text{iso}}$). We show that high-energy dilepton production is sensitive to the plasma isotropization time, τ_{iso} , and can therefore be used to experimentally determine the time of onset for hydrodynamic expansion of a quark-gluon plasma and the magnitude of expected early-time momentum-space anisotropies.

PACS numbers: 11.15Bt, 04.25.Nx, 11.10Wx, 12.38Mh

An important question facing experimentalists and theorists working on heavy-ion experiments ongoing at the Relativistic Heavy Ion Collider (RHIC) and planned at the Large Hadron Collider (LHC) is at what time is it justified to assume that the matter created can be described using simple hydrodynamics. At RHIC energies it has been found that for $p_T \lesssim 2$ GeV the elliptic flow of the matter created is described well by models which assume ideal hydrodynamic behavior starting at very early times $\tau \lesssim 1$ fm/c [1–4]. Since then further refinements including viscous corrections have become available and indications are that the viscosity is constrained to be small [5–7] and results remain consistent with early thermalization of the quark-gluon plasma (QGP). However, given the complexity of solving three-dimensional viscous hydrodynamic equations coupled to a late-time hadronic cascade [8, 9] it would be nice to have an independent way to determine the time at which a QGP begins to undergo hydrodynamic expansion. In this letter we propose to use high-energy dilepton yields as a function of both pair invariant mass and transverse momentum to experimentally determine QGP isotropization time.

The use of ideal hydrodynamics to describe matter requires at a minimum that the matter be isotropic in momentum space [10]. In practical applications it is also necessary to impose an additional constraint (equation-of-state, conformal invariance, etc.) in order to close the resulting system of hydrodynamic equations. When an equation-of-state is applied it is implicitly assumed that the system is isotropic and thermal so that $\tau_{\text{iso}} = \tau_{\text{therm}}$. For simplicity we will also identify these two time scales. Estimates from perturbative QCD for the thermalization time of a QGP range from 2–3 fm/c [11–13]. Recently it has been shown that plasma isotropization is accelerated by unstable plasma modes induced by the rapid longitudinal expansion of the QGP fireball [13, 14]; however, it is still not known by precisely how much.

In most phenomenological treatments of the QGP it is assumed that the plasma thermalizes rapidly with $\tau_{\text{iso}} = \tau_{\text{therm}}$ on the order of the parton formation time. However, given the rapid longitudinal expansion of the matter this seems like a rather strong assumption and one would like to know the effect of momentum-space anisotropies on experimental observables.

Absent a precise dynamical picture of the first few fm/c of the QGP's lifetime we propose a simple phenomenological model for the time-dependence of the plasma momentum-space anisotropy, $\xi = \frac{1}{2} \langle p_T^2 \rangle / \langle p_L^2 \rangle - 1$, and hard momentum scale, p_{hard} . We then use this model to explore the effect of early-time plasma momentum-space anisotropies on high-energy dilepton production. To accomplish this we introduce two parameters: (1) τ_{iso} which is the proper time at which the system begins behaving hydrodynamically and (2) γ which sets the sharpness of the transition to hydrodynamic behavior. For times greater than the parton formation time, τ_0 , but short compared to τ_{iso} we will assume that the system is longitudinally free streaming and for times long compared to τ_{iso} that it is expanding hydrodynamically. To estimate the parton formation time we use the nuclear saturation scale, $\tau_0 \sim Q_s^{-1}$ [15]. For RHIC energies $Q_s \simeq 1.5$ GeV and for LHC energies $Q_s \simeq 2$ GeV implying that $\tau_0 \simeq 0.2$ fm/c and $\tau_0 \simeq 0.1$ fm/c, respectively.

For our final results we present the invariant mass and transverse momentum dependence of medium dilepton production. We compare our results with estimates of other relevant sources and background processes and demonstrate that increasing the QGP isotropization time from $\tau_{\text{iso}} = \tau_0$ to $\tau_{\text{iso}} = 2$ fm/c significantly increases medium high-energy dilepton production. We present detailed calculations of this enhancement and show that at LHC energy it leads to an experimentally measurable effect on dilepton production between $3 \text{ GeV} < M, p_T < 8 \text{ GeV}$.

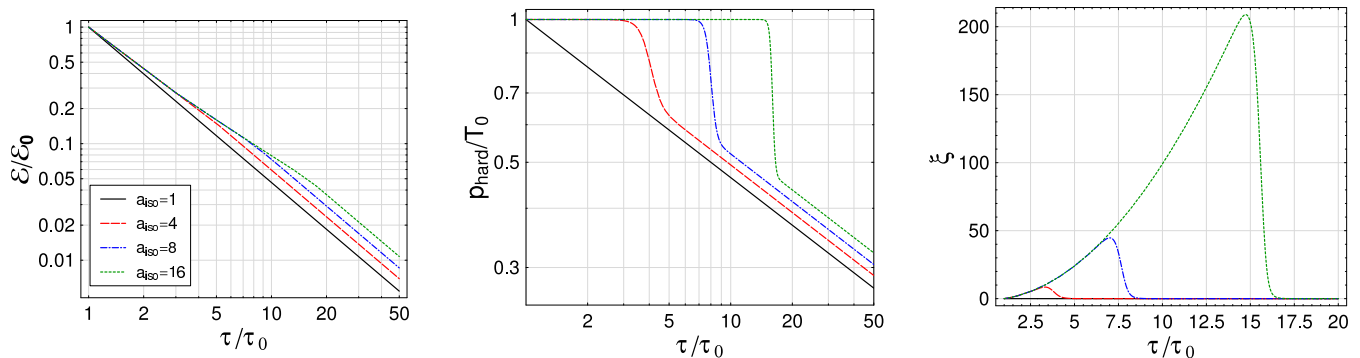


FIG. 1: Model energy density (left), hard momentum scale (middle), and anisotropy parameter (right) for four different isotropization times $\tau_{\text{iso}} \in \{0.1, 0.4, 0.8, 1.6\}$ fm/c assuming $\tau_0 = 0.1$ fm/c. The transition width is taken to be $\gamma = 2$.

DILEPTON RATE

The leading order medium dilepton production rate comes from the annihilation process $q\bar{q} \rightarrow l^+l^-$. Medium dilepton production is computed by folding this rate together with the expected local quark and anti-quark phase space distribution functions [16, 17]. In this work we allow these phase space distribution functions to be anisotropic in momentum-space and then model the time-dependence of the anisotropy. Assuming azimuthal symmetry about the beam (z) axis the time-dependence can be parameterized as

$$f_{\{q,\bar{q}\}}(\mathbf{k}, \tau) = f_{\{q,\bar{q}\},\text{iso}}\left(\sqrt{\mathbf{k}^2 + \xi(\tau)k_z^2}, p_{\text{hard}}(\tau)\right), \quad (1)$$

where $p_{\text{hard}}(\tau)$ is a time-dependent hard momentum scale and $\xi(\tau)$ is a time-dependent parameter reflecting the strength of the local momentum-space anisotropy [18]. We will further assume that f_{iso} is a Fermi-Dirac distribution and that $f_q = f_{\bar{q}}$.

Details of the analytic and numerical calculation of the ξ -dependent rate will be presented elsewhere. Note that for isotropic systems there are appreciable next-to-leading (NLO) order corrections for $E/T \lesssim 1$ [19–22]. When we are sensitive to areas of phase space where there are large NLO corrections we will apply K -factors to our estimates as indicated.

SPACE-TIME MODEL

We now construct a model which interpolates between early-time longitudinal free streaming and late-time ideal hydrodynamic expansion. Given (1) the medium parton energy density can be factorized as

$$\mathcal{E}(p_{\text{hard}}, \xi) = \int \frac{d^3\mathbf{p}}{(2\pi)^3} p f(\mathbf{p}, \xi) = \mathcal{E}_0(p_{\text{hard}}) \mathcal{R}(\xi), \quad (2)$$

where $\mathcal{R}(\xi) = [1/(\xi + 1) + \arctan\sqrt{\xi}/\sqrt{\xi}]/2$ and $\mathcal{E}_0(p_{\text{hard}})$ is the energy density resulting from integra-

tion of the isotropic quark and anti-quark distribution functions appearing in Eq. (1).

Longitudinal Free Streaming Limit: For a longitudinally free streaming plasma $\xi_{\text{FS}}(\tau) = (\tau/\tau_0)^2 - 1$ and p_{hard} is constant and equal to the initial average hard momentum scale in the plasma; therefore, $\mathcal{E}_{\text{FS}}(\tau) = \mathcal{E}(p_{\text{hard}}, \xi_{\text{FS}}(\tau))$. Assuming an isotropic plasma at $\tau = \tau_0$ this results in $p_{\text{hard}}(\tau) = T_0$ and $\lim_{\tau \gg \tau_0} \mathcal{E}_{\text{FS}} \rightarrow \mathcal{E}_0(\tau_0/\tau)$ where T_0 is the initial plasma “temperature”. Note that assuming a formation time of $\tau_0 = 0.1$ fm/c at $\tau = 1$ fm/c we have $\xi_{\text{FS}} \simeq 100$.

Ideal Hydrodynamic Expansion: For a plasma which is undergoing ideal longitudinal hydrodynamic expansion we have $\xi(\tau) = 0$ by assumption. Additionally, since the system is thermal we can identify the hard momentum scale with the plasma temperature so that $p_{\text{hard}}(\tau) = T(\tau) = T_0(\tau_0/\tau)^{1/3}$. Correspondingly, we have $\mathcal{E}_{\text{hydro}} = \mathcal{E}_0(\tau_0/\tau)^{4/3}$.

Interpolating Model: In order to construct a model which interpolates between longitudinal free streaming and hydrodynamic expansion we introduce a smeared step function $\lambda(\tau) \equiv (\tanh[\gamma(\tau - \tau_{\text{iso}})/\tau_0] + 1)/2$. This allows us to model the time-dependence of ξ and p_{hard} as

$$\begin{aligned} \mathcal{E}(\tau) &= \mathcal{E}_{\text{FS}}(\tau) [\mathcal{U}(\tau)/\mathcal{U}(\tau_0)]^{4/3}, \\ p_{\text{hard}}(\tau) &= T_0 [\mathcal{U}(\tau)/\mathcal{U}(\tau_0)]^{1/3}, \\ \xi(\tau) &= a^{2(1-\lambda(\tau))} - 1, \end{aligned} \quad (3)$$

where $\mathcal{U}(\tau) \equiv [\mathcal{R}(a_{\text{iso}}^2 - 1)]^{3\lambda(\tau)/4} (a_{\text{iso}}/a)^{\lambda(\tau)}$, $a \equiv \tau/\tau_0$ and $a_{\text{iso}} \equiv \tau_{\text{iso}}/\tau_0$. The power of \mathcal{R} in \mathcal{U} keeps the energy density continuous at $\tau = \tau_{\text{iso}}$ for all γ .

When $\tau \ll \tau_{\text{iso}}$ we have $\lambda \rightarrow 0$ and the system is longitudinally free streaming. When $\tau \gg \tau_{\text{iso}}$ then $\lambda \rightarrow 1$ and the system is expanding hydrodynamically. In the limit $\gamma \rightarrow \infty$, $\lambda \rightarrow \Theta(\tau - \tau_{\text{iso}})$. In Fig. 1 we plot the time-dependence of \mathcal{E} , p_{hard} , and ξ assuming $\gamma = 2$ for four different plasma isotropization times corresponding to $a_{\text{iso}} \in \{1, 4, 8, 16\}$.

RESULTS

To obtain the final expected dilepton yields we integrate the annihilation rate over $\tau \in \{\tau_0, \tau_f\}$ and $\eta \in \{-2.5, 2.5\}$ with parameters specified by Eq. (3) and τ_f set by $p_{\text{hard}}(\tau_f) = T_c$. In this letter we will present expected e^+e^- yields resulting from a Pb-Pb collision at LHC full beam energy, $\sqrt{s} = 5.5$ TeV. At RHIC energies sensitivity to τ_{iso} is reduced due to the poor signal-to-background ratio for medium dileptons. Predictions for Au-Au at RHIC energy will be presented elsewhere.

In order to facilitate comparison with previous works we take $\tau_0 = 0.088$ fm/c, $T_0 = 845$ MeV, $T_c = 160$ MeV, and $R_T = 7.1$ fm [22]. Here we assume that when the system reaches T_c all medium emission stops. The addition of mixed and hadronic phase emission is not included in the present work since the kinematic range we consider is not sensitive to the late-time evolution of the system (see Fig. 5). In Figs. 2 and 3 we show our final predicted e^+e^- yields as a function of invariant mass and transverse momentum along with predicted yields from other sources. Predictions for Drell-Yan, heavy quark, and jet conversion yields were supplied by the authors of Ref. [22].

As can be seen from Fig. 2 there is a significant variation of the medium dilepton yield when varying the assumed plasma isotropization time from 0.088 fm/c to 2 fm/c. When an isotropization time of 2 fm/c is assumed we see that medium dileptons become as important as Drell-Yan and jet conversion. The reason for the enhanced production is that longitudinal free streaming preserves more transverse momentum than an hydrodynamically expanding plasma. However, all three contributions are down by an order of magnitude from the expected background coming from semileptonic heavy quark decay. In practice this would mean that experimentalists would have to subtract this background to 10%. We note that an indefinitely longitudinally free streaming plasma ($\tau_{\text{iso}} \rightarrow \infty$) produces less low energy ($M, p_T \lesssim 2$ GeV) dileptons due to the rapidly dropping parton densities as $\xi \rightarrow \infty$.

As we show in Fig. 3 as a function of p_T the medium contribution dominates the expected Drell-Yan and jet conversion sources for all $p_T \lesssim 6$ GeV. If an isotropization time of 2 fm/c is assumed then the medium dileptons dominate out to $p_T \sim 9$ GeV. This dominance means that it should be possible to use dilepton production to determine much-needed information about quark-gluon plasma initial conditions at LHC. As can be seen from Fig. 3 at $p_T = 5$ GeV the expected medium dilepton yield varies by nearly an order of magnitude depending on the assumed plasma isotropization time. This level of variation will hopefully be measurable at LHC.

To illustrate the dependence on the model parameter γ in Fig. 4 we have plotted medium dilepton yields obtained

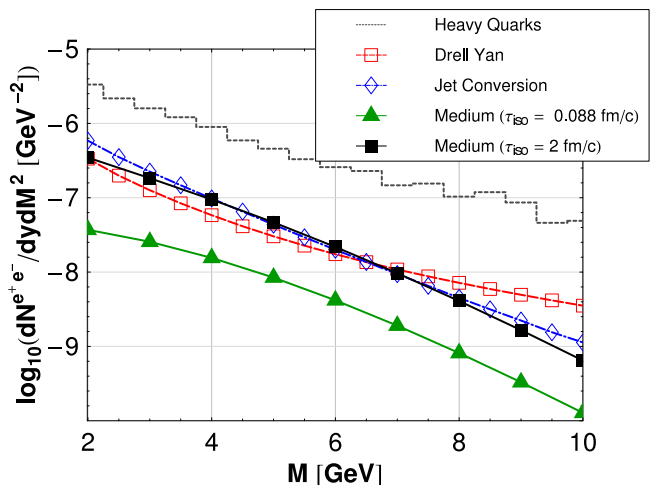


FIG. 2: Dilepton yields as a function of invariant mass with a cut $p_T > 8$ GeV. For medium dileptons we use $\gamma = 2$ and τ_{iso} is taken to be either 0.088 fm/c or 2 fm/c. A K -factor of 1.5 was applied to account for NLO corrections.

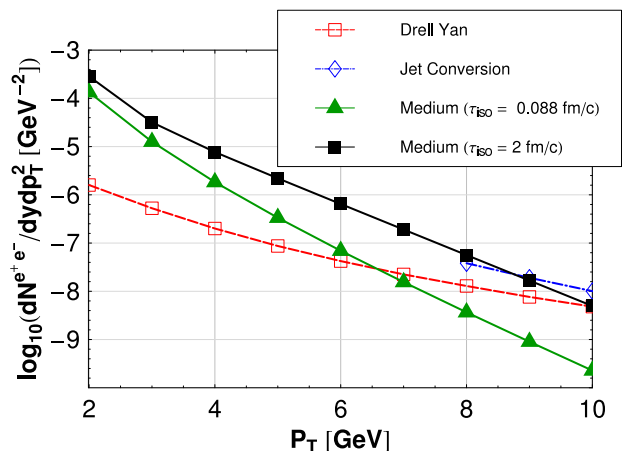


FIG. 3: Dilepton yields as a function of transverse momentum with a cut $0.5 < M < 1$ GeV. For medium dileptons we use $\gamma = 2$ and τ_{iso} is taken to be either 0.088 fm/c or 2 fm/c. A K -factor of 6 was applied to account for NLO corrections.

assuming $\tau_{\text{iso}} = 0.5$ fm/c and $\tau_{\text{iso}} = 2$ fm/c. The central values obtained are with $\gamma = 2$ and the error bars come from variation of γ in the range $0.05 < \gamma < 10$. As can be seen from this Figure between 3 and 8 GeV there is little sensitivity to the parameter γ .

In Fig. 5 we show snapshots of the fraction of medium dileptons produced as a function of transverse momentum. What this figure shows is that by 4 fm/c yields in this kinematic regime are saturated. At 1 fm/c approximately 94% of all $p_T = 4$ GeV dileptons have already been produced as well as 98% of the $p_T = 5$ GeV pairs. This highlights the sensitivity of this observable to early-times after a heavy-ion collision and justifies neglecting the effect of transverse expansion and mixed/hadronic phases when considering dileptons in this kinematic regime.

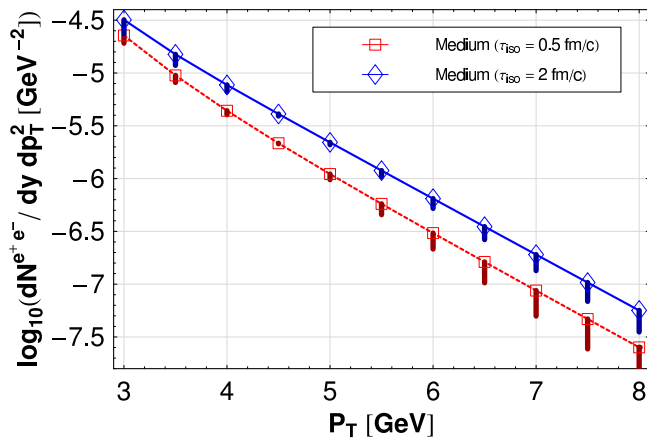


FIG. 4: Dilepton yields as a function of transverse momentum. Shown are yields obtained assuming $\tau_{\text{iso}} = 0.5$ fm/c and 2 fm/c with error bars indicating model variation, $0.05 \leq \gamma \leq 10$. Cuts and K -factor are the same as in Fig. 3.

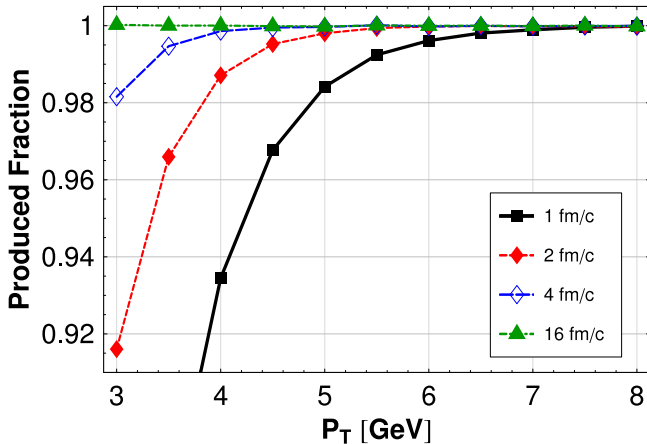


FIG. 5: Fraction of dileptons produced at $\tau \in \{1, 2, 4, 16\}$ fm/c assuming $\tau_{\text{iso}} = 0.5$ fm/c. Cuts are the same as in Fig. 3.

CONCLUSIONS AND DISCUSSION

Based on Figs. 3 and 4 it should be possible to measure τ_{iso} at LHC energies using dilepton production in the kinematic range $3 < p_T < 8$ GeV. Additionally via our model for $\xi(\tau)$ given in Eq. 3 determining τ_{iso} provides an estimate of the maximum amount of momentum-space anisotropy achieved during the lifetime of the QGP.

The effect of varying τ_{iso} is also large in the dilepton spectra vs invariant mass as shown in Fig. 2, however, Drell-Yan and jet conversion production can be up to 10 times larger than medium production making it difficult to measure a clean medium dilepton signal.

Our chief uncertainty is the NLO order corrections to dilepton production incorporating anisotropies. These corrections are particularly important for low-mass dilepton production. At LHC energy it is possible to reduce sensitivity to these NLO corrections by placing cuts $M, p_T \gtrsim 2$ GeV. Another uncertainty comes from our assumption of chemical equilibrium. Naively finite chemi-

cal potentials should affect isotropic and anisotropic plasmas equally so one expects that although the total yields could change one would still see a sensitivity to the assumed isotropization/thermalization time. At leading order in the quark fugacity, λ_q , the ratio of the isotropic to anisotropic rates should be independent of λ_q [23].

Future work will study the effect of finite quark chemical potentials, collisional broadening of the parton distributions, and the possibility of late-time persistent anisotropies (finite viscosity). In addition, models such as (3) can be used to assess the impact of momentum-space anisotropies on other observables.

Acknowledgments

We thank A. Dumitru, A. Ipp, B. Schenke, and S. Turbide. M.M. was supported by the Helmholtz Research School and M.S. by DFG project GR 1536/6-1.

-
- [1] D. Teaney, J. Lauret, and E. V. Shuryak, Phys. Rev. Lett. **86**, 4783 (2001).
 - [2] P. Huovinen, P. F. Kolb, U. W. Heinz, P. V. Ruuskanen, and S. A. Voloshin, Phys. Lett. **B503**, 58 (2001).
 - [3] T. Hirano and K. Tsuda, Phys. Rev. **C66**, 054905 (2002).
 - [4] M. J. Tannenbaum, Rept. Prog. Phys. **69**, 2005 (2006).
 - [5] H.-J. Drescher, A. Dumitru, C. Gombeaud, and J.-Y. Ollitrault, Phys. Rev. **C76**, 024905 (2007).
 - [6] P. Romatschke and U. Romatschke, Phys. Rev. Lett. **99**, 172301 (2007), arXiv:0706.1522 [nucl-th].
 - [7] H. Song and U. W. Heinz, Phys. Lett. **B658**, 279 (2008), arXiv:0709.0742 [nucl-th].
 - [8] C. Nonaka and S. A. Bass, Phys. Rev. **C75**, 014902 (2007).
 - [9] S. A. Bass et al., Prog. Part. Nucl. Phys. **41**, 255 (1998).
 - [10] P. Arnold, J. Lenaghan, G. D. Moore, and L. G. Yaffe, Phys. Rev. Lett. **94**, 072302 (2005), nucl-th/0409068.
 - [11] R. Baier, A. H. Mueller, D. Schiff, and D. T. Son, Phys. Lett. **B502**, 51 (2001), hep-ph/0009237.
 - [12] Z. Xu and C. Greiner, Phys. Rev. **C71**, 064901 (2005), hep-ph/0406278.
 - [13] M. Strickland, J. Phys. **G34**, S429 (2007).
 - [14] S. Mrowczynski and M. H. Thoma, Phys. Rev. **D62**, 036011 (2000), hep-ph/0001164.
 - [15] R. Venugopalan (2007), arXiv:0707.1867 [hep-ph].
 - [16] K. Kajantie, J. I. Kapusta, L. D. McLerran, and A. Mekjian, Phys. Rev. **D34**, 2746 (1986).
 - [17] J. I. Kapusta, L. D. McLerran, and D. Kumar Srivastava, Phys. Lett. **B283**, 145 (1992).
 - [18] P. Romatschke and M. Strickland, Phys. Rev. **D68**, 036004 (2003), hep-ph/0304092.
 - [19] M. H. Thoma and C. T. Traxler, Phys. Rev. **D56**, 198 (1997).
 - [20] P. Arnold, G. D. Moore, and L. G. Yaffe, JHEP **06**, 030 (2002).
 - [21] F. Arleo et al. (2004), hep-ph/0311131.
 - [22] S. Turbide, C. Gale, D. K. Srivastava, and R. J. Fries, Phys. Rev. **C74**, 014903 (2006).
 - [23] M. Strickland, Phys. Lett. **B331**, 245 (1994).